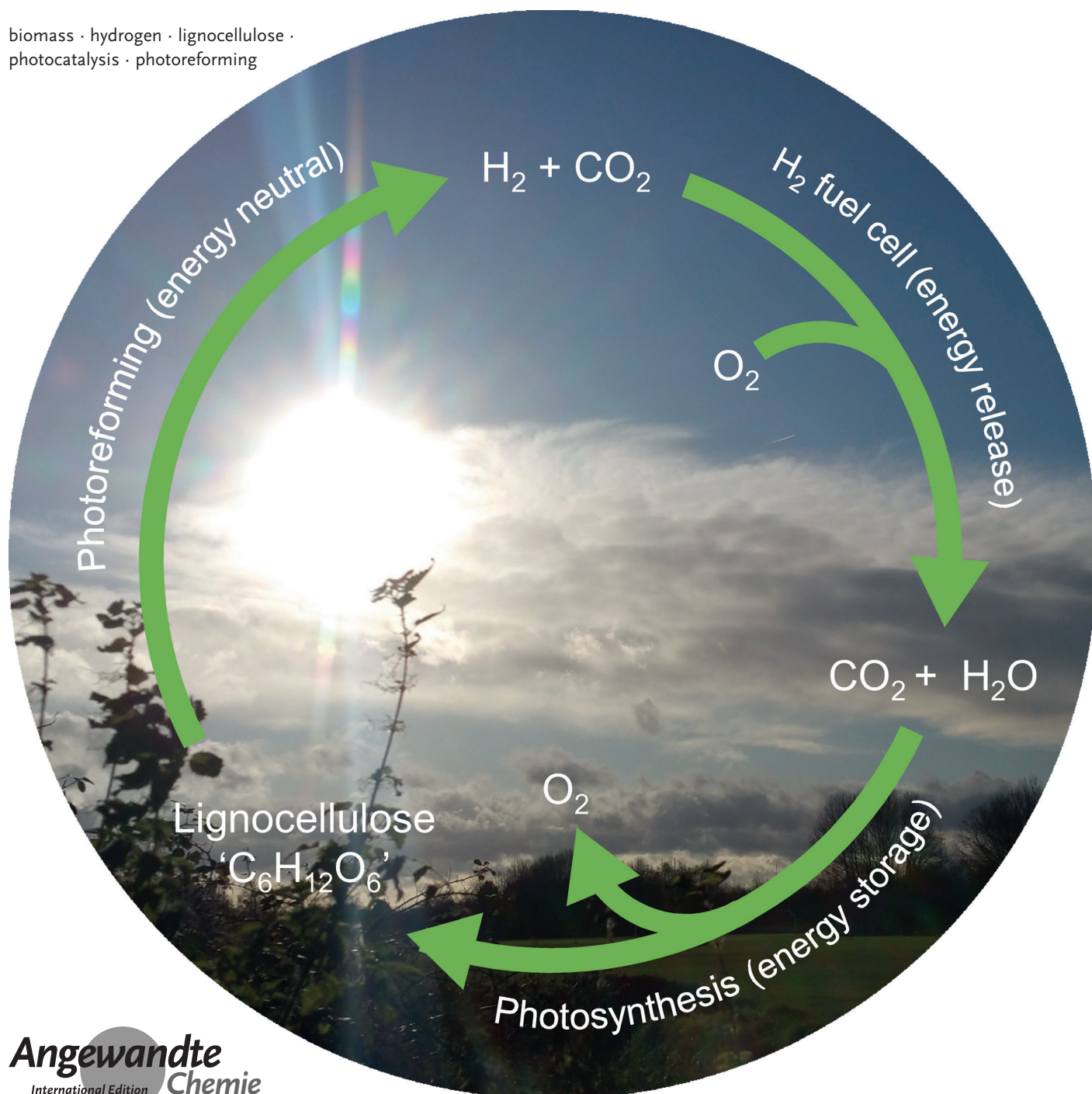


Photoreforming

International Edition: DOI: 10.1002/anie.201710133

German Edition: DOI: 10.1002/ange.201710133

Solar Hydrogen Generation from Lignocellulose

Moritz F. Kuehnel and Erwin Reisner**biomass · hydrogen · lignocellulose ·
photocatalysis · photoreforming

Photocatalytic reforming of lignocellulosic biomass is an emerging approach to produce renewable H_2 . This process combines photo-oxidation of aqueous biomass with photocatalytic hydrogen evolution at ambient temperature and pressure. Biomass conversion is less energy demanding than water splitting and generates high-purity H_2 without O_2 production. Direct photoreforming of raw, unprocessed biomass has the potential to provide affordable and clean energy from locally sourced materials and waste.

1. Introduction

Biomass is Earth's most abundant renewable resource and has been a source of energy to mankind since the Stone Age. Today, our economy depends on fossil fuels, which are derived from ancient biomass. With the gradual consumption of these non-renewable resources and problems associated with CO_2 emission, finding a sustainable source of energy is imperative.^[1] H_2 is a promising energy carrier for a post-fossil era, but current H_2 production relies on fossil fuel reforming and is thus not sustainable.^[2] Generating H_2 fuel directly from waste biomass without the timescales of fossilization has the potential to afford renewable energy at large scale and low cost, without competition with food production.

Lignocellulose is the most abundant form of biomass. It has a multi-component structure, evolved to provide mechanical and chemical stability (Figure 1).^[3] Its primary component, cellulose, forms strong, poorly soluble fibrils comprising linear glucose β -1,4-homopolymer chains linked by hydrogen bonds. Cellulose fibrils are cross-linked by hemicellulose, a branched co-polymer of different pentose and hexose sugars. The major non-carbohydrate component, lignin, is a polyether derived from different phenol monomers in varying compositions. It cross-links the fibril structure and protects it from UV damage.^[4] Lignocellulose utilization is

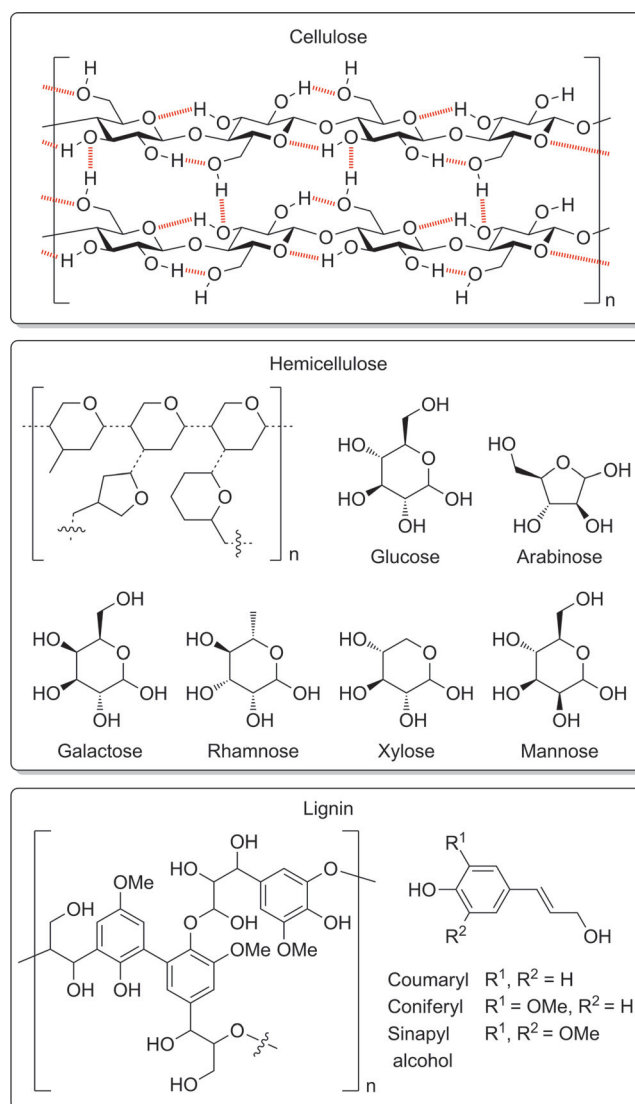


Figure 1. The structural components of lignocellulose.^[3]

therefore kinetically challenging, as it requires disruption of this robust structure.

A number of strategies have been developed to produce fuels directly from biomass.^[5] Alcohol production from combined cellulose saccharification and fermentation is a field of intense research,^[6] but cellulose hydrolysis is slow and

[*] Dr. M. F. Kuehnel, Prof. E. Reisner
 Christian Doppler Laboratory for Sustainable SynGas Chemistry
 Department of Chemistry, University of Cambridge
 Lensfield Road, Cambridge CB2 1EW (UK)
 E-mail: reisner@ch.cam.ac.uk
 Homepage: <http://www-reisner.ch.cam.ac.uk>

Dr. M. F. Kuehnel
 Department of Chemistry
 Swansea University, College of Science
 Singleton Park, Swansea SA2 8PP (UK)
 E-mail: m.f.kuehnel@swansea.ac.uk
 Homepage: <https://moritz-kuehnel.com>

The ORCID identification numbers for the authors of this article can be found under:
<https://doi.org/10.1002/anie.201710133>.

© 2018 The Authors. Published by Wiley-VCH Verlag GmbH & Co. KGaA. This is an open access article under the terms of the Creative Commons Attribution License, which permits use, distribution and reproduction in any medium, provided the original work is properly cited.

separation of the resulting alcohol is uneconomical at low concentrations. Thermochemical processes such as biomass gasification and reforming require high temperatures and pressures, and the generated H_2 contains impurities that must be removed before use.^[7]

2. Photocatalytic Reforming of Biomass

Photocatalytic reforming (PR) of biomass uses the photo-excited state of a semiconductor to drive reforming at ambient conditions (Figure 2A). When the semiconductor

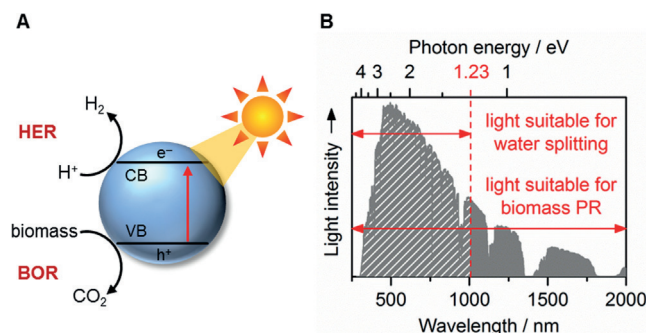


Figure 2. A) Photocatalytic biomass reforming process. B) The solar spectrum as it reaches the earth's surface (AM 1.5G).

absorbs light of energies greater than its band gap, an electron is excited from the valence band (VB) to the conduction band (CB). CB electrons are highly reducing and can promote the fuel-forming hydrogen evolution reaction [HER, Eq. (1)], while the oxidizing holes left in the VB can drive the biomass oxidation reaction [BOR, shown for glucose in Eq. (2)].

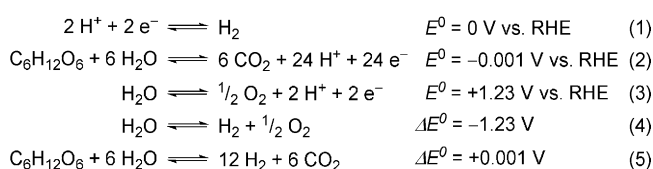
H_2 generation from water splitting [Eqs. (3) and (4)] has a large thermodynamic barrier ($\Delta E^0 = -1.23$ V) due to the energy-demanding oxygen evolution reaction [OER, Eq. (3)]. It also generates explosive mixtures of H_2 and O_2 . In contrast, the overall biomass reforming reaction [Eq. (5)] is almost energy neutral ($\Delta E^0 = +0.001$ V),^[8] meaning energy is only needed to overcome activation barriers. In theory, biomass PR is therefore possible using low-energy photons (visible and IR light), which are highly abundant in the solar spectrum (Figure 2B).



Moritz F. Kuehnel received his PhD from the Freie Universität Berlin (with Dieter Lentz). He was awarded the Schering Prize for his doctoral thesis on carbon-fluorine bond activation. After a postdoctoral stay at the HU Berlin (with Thomas Braun), he joined the group of Erwin Reisner (Cambridge) as a DFG fellow, before his promotion to Senior Postdoc. Recently, he started his independent career as a Chemistry Lecturer at Swansea University. His research encompasses the application of semiconductor nanocrystals for solar fuel production from biomass and CO_2 .



Erwin Reisner obtained his PhD at the University of Vienna (with Bernhard K. Keppler), followed by postdoctoral research at the Massachusetts Institute of Technology (with Stephen J. Lippard) and the University of Oxford (with Fraser A. Armstrong). He is currently the Professor of Energy and Sustainability in the Department of Chemistry at the University of Cambridge, head of the Christian Doppler Laboratory for Sustainable SynGas Chemistry, and director of the UK Solar Fuels Network. His group develops solar-driven chemistry by combining chemical biology, synthetic chemistry and materials chemistry.



Throughout this Minireview, catalyst performance is compared on the basis of the PR rate [$mmol_{H_2} g_{cat}^{-1} h^{-1}$] and external quantum efficiency (EQE). H_2 production is given as yield [$mmol_{H_2} g_{bio}^{-1}$].

3. PR of Lignocellulose Components

Photocatalytic conversion of biomass to CO_2 and H_2 was first reported in 1980 using TiO_2 modified with Pt and RuO_2 as hydrogen evolution and biomass oxidation co-catalysts, respectively.^[9] The field has progressed significantly since then, but the majority of studies are still performed with TiO_2 -based photocatalysts.^[10] While these materials are robust and inexpensive, their large band gaps (3.2 eV) limit solar light utilization to the UV region (Figure 2B). PR studies initially focused on generating H_2 from biomass-derived feedstocks. The higher solubility and reactivity of these feedstocks facilitate reaction kinetics,^[10] but they are valuable chemicals themselves, and thus biomass PR must focus on using inedible waste material without any additional processing.

3.1. Sugars

Sugars have been widely studied as model substrates for biomass photoreforming, since the majority of lignocellulose is based on saccharide monomers (cellulose and hemicellulose).

Glucose PR is most established using Pt/ TiO_2 .^[11] These UV light-absorbing photocatalysts achieved performances up to $1.15 mmol_{H_2} g_{cat}^{-1} h^{-1}$,^[12] and 8.5% EQE.^[11a] Other co-catalysts (Rh,^[13] Ru,^[13b,14] Pd,^[15] Au)^[13b,15b,16] showed enhanced activity, with AuPd/ TiO_2 reaching $8.8 mmol_{H_2} g_{cat}^{-1} h^{-1}$ and 17.5% EQE.^[17] Non-precious co-catalysts (Ni,^[15b,18] Fe,^[19] Cu)^[13a] gave up to $2.0 mmol_{H_2} g_{cat}^{-1} h^{-1}$ and $59 mmol_{H_2} g_{bio}^{-1}$ yield. Performing PR at elevated temperature (30–60 °C)

improved activity^[15a] and allowed quantitative H₂ yield.^[13b,20] Moreover, heteroatom doping (B/N,^[21] S,^[22] F)^[23] or sensitization with upconverting Er:YAlO₃ particles was employed to improve the light absorption of TiO₂.^[24] Pt/TiO₂ also demonstrated PR activity towards other sugars (fructose,^[12c,17,25] galactose,^[26] mannose,^[26a] sorbose,^[26a] arabinose,^[25] xylose^[12d,27]).

Visible-light driven glucose reforming was reported using Pt/CdZnS with rates up to 0.485 mmol_{H₂} g_{cat}⁻¹ h⁻¹,^[28] whereas a related ZnS/ZnIn₂S₄ solid solution offered a lower performance.^[29] Non-precious co-catalysts were shown to be superior over Pt, with a MoS₂/CdS composite^[30] achieving up to 55 mmol_{H₂} g_{cat}⁻¹ h⁻¹ and 9.3 mmol_{H₂} g_{bio}⁻¹ and 81 mmol_{H₂} g_{cat}⁻¹ h⁻¹ reported for Co/CdS/CdO_x quantum dots.^[31] Narrow-band gap metal oxides, such as Zn:Cu₂O (3.82 mmol_{H₂} g_{cat}⁻¹ h⁻¹)^[32] and Fe₂O₃/Si (4.42 mmol_{H₂} g_{cat}⁻¹ h⁻¹)^[33] have shown promising activities for visible-light driven glucose PR. Other suitable materials include LaFeO₃,^[34] Bi_xY_{1-x}VO₄,^[35] CaTa₂O₆,^[36] La:NaTaO₃,^[37] and SrTiO₃.^[38]

3.2. Oligosaccharides and Polysaccharides

Disaccharides (cellobiose,^[25,26] maltose,^[26b,34b] sucrose,^[9,11a,12a,b,13b,21,26a,39] lactose)^[26b] generally gave lower PR rates than monosaccharides, with a maximum activity of 3.69 mmol_{H₂} g_{cat}⁻¹ h⁻¹ reported for sucrose PR over Pt/B,N:TiO₂ and a maximum yield of 20 mmol_{H₂} g_{bio}⁻¹ over Pd/TiO₂.^[13b] PR of soluble polysaccharides proceeded at even lower rates,^[9,12c,26b] presumably due to their higher molecular weights and stable hydrogen-bonded structures. Soluble starch gave 3.14 mmol_{H₂} g_{cat}⁻¹ h⁻¹ and 26 mmol_{H₂} g_{bio}⁻¹ yield over Pd/TiO₂^[13b] and 1.8% EQE over Pt/TiO₂.^[11a] Visible-light driven PR of polysaccharides has only been investigated for hemicellulose with Co/CdS/CdO_x, with a rate of 2.04 mmol_{H₂} g_{cat}⁻¹ h⁻¹.^[31]

3.3. Cellulose

Only a handful of examples have demonstrated cellulose PR. While the thermodynamics of cellulose reforming are similar to that of oligosaccharides,^[40] the kinetics are more challenging due to the compact tertiary structure of cellulose.

Direct cellulose PR was first demonstrated using Pt/TiO₂/RuO₂ at low activities (0.012 mmol_{H₂} g_{cat}⁻¹ h⁻¹);^[9] comparable performance was achieved with Pt/TiO₂.^[11a] Improved cellulose solubility at alkaline conditions led to enhanced activity (0.041 mmol_{H₂} g_{cat}⁻¹ h⁻¹) and 1.3% EQE.^[9,11b] Optimization of catalyst loading, cellulose concentration, and pH further increased the performance of Pt/TiO₂ to 0.223 mmol_{H₂} g_{cat}⁻¹ h⁻¹.^[41] Remarkably, cellulose photoreforming proceeded with comparable activity under natural sunlight, demonstrating real-world applicability. Immobilizing cellulose on the photocatalyst surface enhanced the rate of photocatalysis and produced 67 mmol_{H₂} g_{bio}⁻¹ under UV light; 14 mmol_{H₂} g_{bio}⁻¹ yield were produced under natural sunlight.^[42] Further enhancement was reported upon raising the

reaction temperature (0.61 mmol_{H₂} g_{cat}⁻¹ h⁻¹ at 40°C).^[26b] An inexpensive Ni/TiO₂ photocatalyst achieved a performance of 0.12 mmol_{H₂} g_{cat}⁻¹ h⁻¹ at 60°C.^[15b] Visible-light driven cellulose PR was reported at Co/CdS/CdO_x in alkaline solution with rates up to 4.9 mmol_{H₂} g_{cat}⁻¹ h⁻¹ and 7.4 mmol_{H₂} g_{bio}⁻¹.^[31]

3.4. Lignin

Although lignin is considered a promising renewable feedstock,^[43] it has received little attention as a PR substrate. Lignin PR is hampered by its redox stability and brown color, limiting light absorption by the photocatalyst. Pt/TiO₂ generated 0.026 mmol_{H₂} g_{cat}⁻¹ h⁻¹ from lignin under UV light (0.6% EQE).^[44] Visible-light driven lignin PR was reported using CdS/CdO_x (0.26 mmol_{H₂} g_{cat}⁻¹ h⁻¹)^[31] and C,N,S-doped ZnO/ZnS.^[45]

4. Raw Biomass PR

Direct PR of unprocessed biomass is highly desirable to lower H₂ production cost, but is hampered by low substrate solubility. Light is scattered from insoluble biomass and absorbed by colored components. The recalcitrance of raw biomass causes a large overpotential for the BOR reaction, requiring strongly oxidizing VB holes.

PR of various plants (Table 1) was first shown over Pt/TiO₂ at rates comparable to pure cellulose (0.004–0.018 mmol_{H₂} g_{cat}⁻¹ h⁻¹).^[11a,b] Enhanced performance was achieved in alkaline solution, or upon addition of the OER catalyst RuO₂ (0.058 mmol_{H₂} g_{cat}⁻¹ h⁻¹). Elevated temperatures (60°C) allowed PR of Fescue grass over Pt/TiO₂ at 0.061 mmol_{H₂} g_{cat}⁻¹ h⁻¹, albeit only after removal of chlorophyll.^[15b] Natural sunlight-driven PR of plant matter proceeds in neutral water at rates up to 0.095 mmol_{H₂} g_{cat}⁻¹ h⁻¹ over Pt/TiO₂.^[41] H₂ yields were found to vary widely across the different types of biomass (Table 1), with aquatic plants generally demonstrating higher rates and yields than terrestrial plants under similar conditions, presumably due to their lower lignin content. 3.3 mmol_{H₂} g_{bio}⁻¹ were produced from laver with 3.3% EQE.^[11a] A visible-light absorbing Co/CdS/CdO_x photocatalyst showed high PR activity under simulated sunlight.^[31] Bagasse, wood, grass and sawdust gave H₂ production rates and yields of up to 5.3 mmol_{H₂} g_{cat}⁻¹ h⁻¹ and 0.49 mmol_{H₂} g_{bio}⁻¹. Strongly alkaline conditions enhanced biomass solubility and photocatalyst stability.

Biomass solubility is crucial for high PR performance. Adding detergents was shown to enhance the PR rate of castor oil at aqueous Pt/TiO₂.^[46] PR of cotton subjected to hydrothermal liquefaction (250°C, 40 bar)^[47] was 50 times faster than with untreated cotton under similar conditions,^[11b] but the overall H₂ yield was lower. Dilute acid hydrolysis of pinewood (160°C, 10 bar) gave a hydrolysate suitable for high-yield PR over Pt/TiO₂ (0.813 mmol_{H₂} g_{bio}⁻¹).^[48] Alternatively, raw biomass can be digested at mild conditions using natural enzymes. PR of various cellulase/xylanase-treated grasses^[27,49] over Pt/TiO₂ achieved rates up to 1.9 mmol_{H₂} g_{cat}⁻¹ h⁻¹ and a yield of 34.6 mmol_{H₂} g_{bio}⁻¹. Protease

Table 1: Selected examples of photocatalytic reforming of unprocessed lignocellulose.

Substrate	Catalyst	Rate [mmol _{H₂} g _{cat} ⁻¹ h ⁻¹]	Yield [mmol _{H₂} g _{bio} ⁻¹]	EQE [%]	Conditions	Light source	Reference
cherry wood	4% Pt/TiO ₂	0.049	0.296 (10 h)	1.1	5 M KOH	Xe	[11b]
wooden branch	Co/CdS/CdO _x	5.31	0.49 (24 h)	n/a	10 M KOH, 25°C	AM 1.5	[31]
sawdust	Co/CdS/CdO _x	0.75	0.070 (24 h)	n/a	10 M KOH, 25°C	AM 1.5	[31]
Dutch clover	4% Pt/TiO ₂	0.047	0.284 (10 h)	1.1	5 M KOH	Xe	[11b]
goldenrod	4% Pt/TiO ₂	0.018	0.11 (10 h)	0.4	5 M KOH	Xe	[11b]
rice plant	5% Pt/TiO ₂	0.058	1.75 (10 h)	1.3	5 M KOH	Xe	[11a]
rice husk	0.5% Pt/TiO ₂	0.095	n/a	n/a	H ₂ O	sunlight	[41]
alfalfa stems	0.5% Pt/TiO ₂	0.100	n/a	n/a	H ₂ O	UV	[41]
turf	5% Pt/TiO ₂	0.033	0.98 (10 h)	0.74	5 M KOH	Xe	[11a]
fescue grass	0.2% Pt/TiO ₂	0.061	0.076 (3 h)	n/a	H ₂ O, 60°C	Xe	[15b]
grass	Co/CdS/CdO _x	1.0	0.093 (24 h)	n/a	10 M KOH, 25°C	AM 1.5	[31]
bagasse	Co/CdS/CdO _x	0.37	0.034 (24 h)	n/a	10 M KOH, 25°C	AM 1.5	[31]
water hyacinth	4% Pt/TiO ₂	0.034	0.202 (10 h)	0.7	5 M KOH	Xe	[11b]
wakame seaweed	4% Pt/TiO ₂	0.055	0.332 (10 h)	1.2	5 M KOH	Xe	[11b]
<i>chlorella</i> algae	5% Pt/TiO ₂	0.090	2.7 (10 h)	2.0	5 M KOH	Xe	[11a]
laver	5% Pt/TiO ₂	0.111	3.32 (10 h)	3.3	5 M KOH	Xe	[11a]

A-digested *chlorella* produced 30 mmol_{H₂} g_{bio}⁻¹ at rates up to 0.234 mmol_{H₂} g_{cat}⁻¹ h⁻¹[50] in neutral water (cf. 0.73 mmol_{H₂} g_{bio}⁻¹ and 0.024 mmol_{H₂} g_{cat}⁻¹ h⁻¹ for untreated *chlorella* under these conditions).[11a] Although the yields and rates of pre-treated biomass compare favorably to PR without pre-treatment, pre-processing adds considerable cost and time to the overall process.

5. The PR Mechanism

Photoreforming consists of two separate half-reactions (see Section 2). HER is substrate-independent, and typically proceeds at metal co-catalysts such as Pt. This co-catalyst acts both as a Schottky barrier that suppresses charge recombination and as a HER catalyst. PR in D₂O has shown that the generated H₂ originates from the aqueous solvent rather than the biomass.[11,31]

BOR is a more complex multi-step process that directly involves the substrate. PR rates with various substrates differ

depending on the substrates' adsorption to the photocatalyst surface.[11c,12a,13b,28b,42,51] This is consistent with the Langmuir-type kinetics observed for glucose PR on TiO₂. [13b,15a] Infrared (IR) spectroscopy,[51a] electron energy loss spectroscopy (EELS)[51a] and X-ray absorption near edge structure (XANES)[52] measurements confirm that glucose chemisorbs on TiO₂. Improving this binding by changing the ionic strength,[28b] using α-glucose instead of β-glucose,[53] or immobilizing the substrate[42] enhances the PR rate. Chemisorption promotes electronic interactions such as substrate-photocatalyst charge transfer,[51a] shifting the flat band potential[11c,12a] and hole trapping at the substrate.[54] BOR is therefore believed to involve direct hole transfer to the chemisorbed substrate (Figure 3A),[51b,52,54] generating surface-bound radicals on the sub-ns timescale, as evidenced for glucose by transient absorption spectroscopy (TAS)[52] and electron paramagnetic resonance (EPR)[55] spectroscopy. Fragmentation of these radicals leads to C–C bond cleavage starting from C₁,[55] resulting in a step-wise degradation of glucose to arabinose, erythrose etc. with concomitant formic

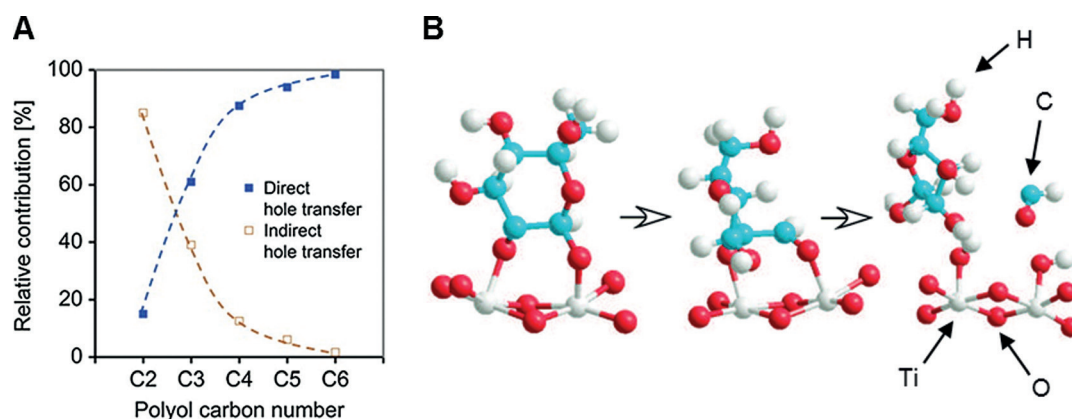


Figure 3. Mechanism of biomass PR on metal-oxide surfaces. A) Mechanistic pathway depending on the substrate reproduced from Ref. [51b] with permission from Elsevier. B) Mechanistic proposal for glucose reforming on TiO₂ reproduced from Ref. [55] with permission from the ACS.

acid formation (Figure 3B).^[13c] Metal co-catalysts can be involved in BOR, presumably by interaction with chemisorbed intermediates.^[51c]

Alternatively, involvement of OH[•] radicals has been suggested^[15b,30,34a,41] on the basis of spin-trapping EPR experiments in the absence of biomass.^[14,23,29] However, biomass PR is known to proceed on photocatalysts incapable of generating OH[•] radicals.^[13c,31]

6. Biomass PR Beyond H₂ Generation

The low market value of H₂ renders alternative PR products desirable and, consequently, the selective photocatalytic transformation of renewable feedstocks into valuable organic products is a field of intense research.^[56] The radical nature of glucose PR over M/TiO₂ gives rise to a number of trace by-products such as CO,^[12e,14] CH₄,^[14,19,22] formic acid^[16] and others.^[19] PR of cellulose or raw biomass over Pt/TiO₂ generated traces of C₂H₆, ethanol and acetone.^[11b] Polymorph-dependent selectivity control was observed in glucose PR over Rh/TiO₂. Rutile showed preferred decarboxylation of glucose to give arabinose and erythrose, while further oxidation to CO₂ was suppressed.^[13c] LaFeO₃ produced only H₂ and gluconate,^[34b] because further oxidation was slow on the less oxidizing VB compared to TiO₂. Impregnating Pt/TiO₂ with cellulose promoted glucose, cellobiose and formic acid formation during PR.^[42] The produced glucose could be further photoreformed at Pt/TiO₂ to hydroxymethyl furfural.^[41] Accumulation of formate was seen during cellulose PR at CdS/CdO_x,^[31] as formic acid PR was slower than cellulose PR. Formic acid could be further photoreformed at CdS to H₂ or CO.^[57]

Alternatively, reducing equivalents generated upon biomass photo-oxidation can be used for organic transformations instead of H₂ generation. Photocatalytic conversion of glucose to arabinose and erythrose over Pd/TiO₂ could be coupled with the reduction of nitroarenes and aldehydes to anilines and alcohols, respectively, thus producing high-value products from both half-reactions.^[58] This approach was recently adapted using lignin as both reductant and oxidant.^[59] Photo-oxidation of lignin alcohol moieties to ketones with simultaneous reductive C–O bond cleavage in the lignin backbone resulted in an overall transfer hydrogenolysis of lignin to substituted phenols.

7. Conclusion and Outlook

Biomass PR is a promising approach to sustainably generate fuels and feedstock chemicals. The simplicity of this room-temperature process to produce clean H₂ fuel is of considerable advantage over thermochemical methods, but efficiencies are yet to match conventional processes. This field has historically focused on materials and catalysts designed for solar water splitting, limiting photocatalytic activity to UV light. Future work should focus on designing narrow band-gap materials specifically for biomass PR to enhance the performance under natural sunlight. Tailor-made biomass oxidation

catalysts will be needed to lower the required driving force and to improve the selectivity towards high-value products. Ultimately, integrating PR with other solar fuel production systems by utilizing low-energy photons unsuitable for water splitting may be the key to translate PR into a scalable and economically viable process.

Acknowledgements

This work was supported by the Christian Doppler Research Association (Austrian Federal Ministry of Science, Research and Economy and the National Foundation for Research, Technology and Development), the OMV Group and the EPSRC (IAA Follow-on fund). We thank Wolfgang Hofer (OMV), Dr. David W. Wakerley, Taylor Uekert, and Daniel Antón García (University of Cambridge) for helpful discussions.

Conflict of interest

A patent covering biomass photoreforming has been filed by Cambridge Enterprise (PCT/EP2017/080371) that names M.F.K. and E.R. as inventors.

How to cite: *Angew. Chem. Int. Ed.* **2018**, *57*, 3290–3296
Angew. Chem. **2018**, *130*, 3346–3353

- [1] IPCC, *Climate Change 2013: The Physical Science Basis* (Eds.: T. F. Stocker, D. Qin, G.-K. Plattner, M. M. B. Tignor, S. K. Allen, J. Boschung, A. Nauels, Y. Xia, V. Bex, P. M. Midgley), Cambridge University Press, Cambridge, **2013**.
- [2] I. Dincer, C. Acar, *Int. J. Hydrogen Energy* **2015**, *40*, 11094–11111.
- [3] F. H. Isikgor, C. R. Becer, *Polym. Chem.* **2015**, *6*, 4497–4559.
- [4] S.-H. Li, S. Liu, J. C. Colmenares, Y.-J. Xu, *Green Chem.* **2016**, *18*, 594–607.
- [5] S. Zinoviev, F. Müller-Langer, P. Das, N. Bertero, P. Fornasiero, M. Kaltschmitt, G. Centi, S. Miertus, *ChemSusChem* **2010**, *3*, 1106–1133.
- [6] G. P. Robertson, S. K. Hamilton, B. L. Barham, B. E. Dale, R. C. Izaurralde, R. D. Jackson, D. A. Landis, S. M. Swinton, K. D. Thelen, J. M. Tiedje, *Science* **2017**, *356*, eaal2324.
- [7] R. M. Navarro, M. C. Sánchez-Sánchez, M. C. Alvarez-Galvan, F. del Valle, J. L. G. Fierro, *Energy Environ. Sci.* **2009**, *2*, 35–54.
- [8] *CRC Handbook of Chemistry and Physics, 95th ed.* (Ed.: W. M. Haynes), CRC, Taylor and Francis, Boca Raton, **2015**.
- [9] T. Kawai, T. Sakata, *Nature* **1980**, *286*, 474–476.
- [10] A. V. Puga, *Coord. Chem. Rev.* **2016**, *315*, 1–66.
- [11] a) T. Kawai, T. Sakata, *Chem. Lett.* **1981**, *10*, 81–84; b) T. Sakata, T. Kawai, *Nouv. J. Chim.* **1981**, *5*, 279–281; c) M. R. St. John, A. J. Furgala, A. F. Sammells, *J. Phys. Chem.* **1983**, *87*, 801–805.
- [12] a) Y.-X. Li, Y.-Z. Xie, S.-Q. Peng, *Chem. J. Chin. Univ.* **2007**, *28*, 156–158; b) H. Bahruji, M. Bowker, P. R. Davies, L. S. Al-Mazroai, A. Dickinson, J. Greaves, D. James, L. Millard, F. Pedrono, *J. Photochem. Photobiol. A* **2010**, *216*, 115–118; c) S. Deguchi, N. Shibata, T. Takeichi, Y. Furukawa, N. Isu, *Jpn. Pet. Inst.* **2010**, *53*, 95–100; d) T. Shiragami, T. Tomo, H. Tsumagari, R. Yuki, T. Yamashita, M. Yasuda, *Chem. Lett.* **2012**, *41*, 29–31; e) Q. Xu, Y. Ma, J. Zhang, X. Wang, Z. Feng, C. Li, *J. Catal.* **2011**, *278*, 329–335.

- [13] a) G. Wu, T. Chen, G. Zhou, X. Zong, C. Li, *Sci. China Ser. B* **2008**, *51*, 97–100; b) X. Fu, J. Long, X. Wang, D. Y. C. Leung, Z. Ding, L. Wu, Z. Zhang, Z. Li, X. Fu, *Int. J. Hydrogen Energy* **2008**, *33*, 6484–6491; c) R. Chong, J. Li, Y. Ma, B. Zhang, H. Han, C. Li, *J. Catal.* **2014**, *314*, 101–108.
- [14] Q. Gu, J. Long, L. Fan, L. Chen, L. Zhao, H. Lin, X. Wang, *J. Catal.* **2013**, *303*, 141–155.
- [15] a) P. Gomathisankar, D. Yamamoto, H. Katsumata, T. Suzuki, S. Kaneco, *Int. J. Hydrogen Energy* **2013**, *38*, 5517–5524; b) A. Caravaca, W. Jones, C. Hardacre, M. Bowker, *Proc. R. Soc. A* **2016**, *472*, 20160054.
- [16] F. Gärtner, S. Losse, A. Boddien, M.-M. Pohl, S. Denurra, H. Junge, M. Beller, *ChemSusChem* **2012**, *5*, 530–533.
- [17] R. Su, R. Tiruvalam, A. J. Logsdail, Q. He, C. A. Downing, M. T. Jensen, N. Dimitratos, L. Kesavan, P. P. Wells, R. Bechstein, H. H. Jensen, S. Wendt, C. R. A. Catlow, C. J. Kiely, G. J. Hutchings, F. Besenbacher, *ACS Nano* **2014**, *8*, 3490–3497.
- [18] R. M. Mohamed, E. S. Aazam, *Chin. J. Catal.* **2012**, *33*, 247–253.
- [19] S. Mozia, A. Kułagowska, A. W. Morawski, *Molecules* **2014**, *19*, 19633–19647.
- [20] J. C. Colmenares, A. Magdziarz, M. A. Aramendia, A. Marinas, J. M. Marinas, F. J. Urbano, J. A. Navio, *Catal. Commun.* **2011**, *16*, 1–6.
- [21] N. Luo, Z. Jiang, H. Shi, F. Cao, T. Xiao, P. P. Edwards, *Int. J. Hydrogen Energy* **2009**, *34*, 125–129.
- [22] V. Vaiano, G. Iervolino, G. Sarno, D. Sannino, L. Rizzo, J. J. Murcia Mesa, M. C. Hidalgo, J. A. Navio, *Oil Gas Sci. Technol. Rev. IFP Energies nouvelles* **2015**, *70*, 891–902.
- [23] J. Yu, L. Qi, M. Jaroniec, *J. Phys. Chem. C* **2010**, *114*, 13118–13125.
- [24] C. Ma, Y. Li, H. Zhang, Y. Chen, C. Lu, J. Wang, *Chem. Eng. J.* **2015**, *273*, 277–285.
- [25] C. G. Silva, M. J. Sampaio, R. R. N. Marques, L. A. Ferreira, P. B. Tavares, A. M. T. Silva, J. L. Faria, *Appl. Catal. B* **2015**, *178*, 82–90.
- [26] a) M. Yasuda, R. Kurogi, T. Matsumoto, *Res. Chem. Intermed.* **2016**, *42*, 3919–3928; b) D. I. Kondarides, V. M. Daskalaki, A. Patsoura, X. E. Verykios, *Catal. Lett.* **2008**, *122*, 26–32.
- [27] M. Yasuda, R. Kurogi, H. Tsumagari, T. Shiragami, T. Matsumoto, *Energies* **2014**, *7*, 4087–4097.
- [28] a) S.-Q. Peng, Y.-J. Peng, Y.-X. Li, G.-X. Lu, S.-B. Li, *Res. Chem. Intermed.* **2009**, *35*, 739–749; b) Y. Li, D. Gao, S. Peng, G. Lu, S. Li, *Int. J. Hydrogen Energy* **2011**, *36*, 4291–4297.
- [29] Y. Li, J. Wang, S. Peng, G. Lu, S. Li, *Int. J. Hydrogen Energy* **2010**, *35*, 7116–7126.
- [30] C. Li, H. Wang, J. Ming, M. Liu, P. Fang, *Int. J. Hydrogen Energy* **2017**, *42*, 16968–16978.
- [31] D. W. Wakerley, M. F. Kuehnel, K. L. Orchard, K. H. Ly, T. E. Rosser, E. Reisner, *Nat. Energy* **2017**, *2*, 17021.
- [32] a) L. Zhang, D. Jing, L. Guo, X. Yao, *ACS Sustainable Chem. Eng.* **2014**, *2*, 1446–1452; b) L. Zhang, J. Shi, M. Liu, D. Jing, L. Guo, *Chem. Commun.* **2014**, *50*, 192–194.
- [33] G. Carraro, C. Maccato, A. Gasparotto, T. Montini, S. Turner, O. I. Lebedev, V. Gombac, G. Adami, G. Van Tendeloo, D. Barreca, P. Fornasiero, *Adv. Funct. Mater.* **2014**, *24*, 372–378.
- [34] a) G. Iervolino, V. Vaiano, D. Sannino, L. Rizzo, P. Ciambelli, *Int. J. Hydrogen Energy* **2016**, *41*, 959–966; b) G. Iervolino, V. Vaiano, D. Sannino, L. Rizzo, V. Palma, *Appl. Catal. B* **2017**, *207*, 182–194.
- [35] D. Jing, M. Liu, J. Shi, W. Tang, L. Guo, *Catal. Commun.* **2010**, *12*, 264–267.
- [36] P. Wang, P. Weide, M. Muhler, R. Marschall, M. Wark, *APL Mater.* **2015**, *3*, 104412.
- [37] X. Fu, X. Wang, D. Y. C. Leung, W. Xue, Z. Ding, H. Huang, X. Fu, *Catal. Commun.* **2010**, *12*, 184–187.
- [38] T. Puangpetch, T. Sreethawong, S. Yoshikawa, S. Chavadej, *J. Mol. Catal. A* **2009**, *312*, 97–106.
- [39] M. Ilie, B. Cojocaru, V. I. Parvulescu, H. Garcia, *Int. J. Hydrogen Energy* **2011**, *36*, 15509–15518.
- [40] Y. B. Tewari, B. E. Lang, S. R. Decker, R. N. Goldberg, *J. Chem. Thermodyn.* **2008**, *40*, 1517–1526.
- [41] A. Speltini, M. Sturini, D. Dondi, E. Annovazzi, F. Maraschi, V. Caratto, A. Profumo, A. Buttafava, *Photochem. Photobiol. Sci.* **2014**, *13*, 1410–1419.
- [42] G. Zhang, C. Ni, X. Huang, A. Welgamage, L. A. Lawton, P. K. J. Robertson, J. T. S. Irvine, *Chem. Commun.* **2016**, *52*, 1673–1676.
- [43] T. Renders, S. Van den Bosch, S.-F. Koelewijn, W. Schutyser, B. F. Sels, *Energy Environ. Sci.* **2017**, *10*, 1551–1557.
- [44] T. Sakata, T. Kawai, *J. Synth. Org. Chem. Jpn.* **1981**, *39*, 589–602.
- [45] S. R. Kadam, V. R. Mate, R. P. Panmand, L. K. Nikam, M. V. Kulkarni, R. S. Sonawane, B. B. Kale, *RSC Adv.* **2014**, *4*, 60626–60635.
- [46] S. Deguchi, T. Takeichi, S. Shimasaki, M. Ogawa, N. Isu, *AIChE J.* **2011**, *57*, 2237–2243.
- [47] A. Shende, R. Tungal, R. Jaswal, R. Shende, *Am. J. Ener. Res.* **2015**, *3*, 1–7.
- [48] R. Jaswal, R. Shende, W. Nan, A. Shende, *Int. J. Hydrogen Energy* **2017**, *42*, 2839–2848.
- [49] a) T. Shiragami, T. Tomo, H. Tsumagari, Y. Ishii, M. Yasuda, *Catalysts* **2012**, *2*, 56–67; b) M. Yasuda, Misriyani, Y. Takenouchi, R. Kurogi, S. Uehara, T. Shiragami, *J. Sustainable Bioenergy Syst.* **2015**, *5*, 1–9.
- [50] M. Yasuda, S. Hirata, T. Matsumoto, *J. Jpn. Inst. Energy* **2016**, *95*, 599–604.
- [51] a) G. Kim, S.-H. Lee, W. Choi, *Appl. Catal. B* **2015**, *162*, 463–469; b) K. E. Sanwald, T. F. Berto, W. Eisenreich, O. Y. Gutiérrez, J. A. Lercher, *J. Catal.* **2016**, *344*, 806–816; c) H. Bahruji, M. Bowker, P. R. Davies, F. Pedrono, *Appl. Catal. B* **2011**, *107*, 205–209.
- [52] I. A. Shkrob, M. C. Sauer, Jr., D. Gosztola, *J. Phys. Chem. B* **2004**, *108*, 12512–12517.
- [53] M. Zhou, Y. Li, S. Peng, G. Lu, S. Li, *Catal. Commun.* **2012**, *18*, 21–25.
- [54] M.-H. Du, J. Feng, S. B. Zhang, *Phys. Rev. Lett.* **2007**, *98*, 066102.
- [55] I. A. Shkrob, T. W. Marin, S. D. Chemerisov, M. D. Sevilla, *J. Phys. Chem. C* **2011**, *115*, 4642–4648.
- [56] a) *Heterogeneous Photocatalysis: From Fundamentals to Green Applications* (Eds.: J. C. Colmenares, Y.-J. Xu), Springer, Berlin, **2016**; b) J. C. Colmenares in *Green Photo-active Nanomaterials: Sustainable Energy and Environmental Remediation* (Eds.: N. Nuraje, R. Asmatulu, G. Mul), The Royal Society of Chemistry, **2016**, pp. 168–201.
- [57] M. F. Kuehnel, D. W. Wakerley, K. L. Orchard, E. Reisner, *Angew. Chem. Int. Ed.* **2015**, *54*, 9627–9631; *Angew. Chem.* **2015**, *127*, 9763–9767.
- [58] B. Zhou, J. Song, H. Zhou, T. Wu, B. Han, *Chem. Sci.* **2016**, *7*, 463–468.
- [59] N. Luo, M. Wang, H. Li, J. Zhang, T. Hou, H. Chen, X. Zhang, J. Lu, F. Wang, *ACS Catal.* **2017**, *7*, 4571–4580.

Manuscript received: September 30, 2017

Accepted manuscript online: December 8, 2017

Version of record online: February 5, 2018